JAAS

ROYAL SOCIETY OF CHEMISTRY

PAPER

View Article Online
View Journal

Cite this: DOI: 10.1039/d3ja00353a

Barite oxygen isotope reference materials for highly precise and accurate SIMS microanalysis†

Lan-Lan Tian, [a] Yue Guan,[a] Wen-Li Xie,[a] Kexin Xu,[a] Feng-Tai Tong,[b] Tao Yang, [a] Yong-Bo Peng[b] and Xiao-Lei Wang *[a]

Received 18th October 2023
Accepted 29th February 2024

DOI: 10.1039/d3ja00353a

rsc.li/jaas

Barite is an important record of marine sulfate evolution throughout geologic history. Variations in oxygen isotope compositions ($\delta^{18}O$) at the microscale are highly important for studying the evolution of marine sulfate. However, the application of this proxy has been hindered due to the lack of reference materials for secondary ion mass spectrometry (SIMS) microanalysis. This study introduces two new potential reference materials, NJU-Ba-1 and FJ barite for microbeam oxygen isotope measurements. Detailed examinations of the texture and major elements revealed no internal zoning of ground fragments from the two barite reference materials. The recommended $\delta^{18}O_{VSMOW}$ values of NJU-Ba-1 and FJ were determined by gas-source isotope ratio mass spectrometry (GS-IRMS), with results of 7.94 ± 0.30‰ (2SD, $N = 11$) and 7.52 ± 0.34‰ (2SD, $N = 8$), respectively. SIMS instrumental stability was monitored by analyses of well characterized zircon references (Penglai and Qinghu), and the robustness of the SIMS barite $\delta^{18}O$ measurements was further assessed by comparison with the values recommended by GS-IRMS. The effects of the crystallographic orientation, topography, and X–Y position on SIMS barite $\delta^{18}O$ measurement were also examined. Multiple SIMS analyses suggest that both NJU-Ba-1 and FJ barite are homogeneous in oxygen isotope composition at the ~20 μm level, with two standard deviations (2SD) of 0.36‰ ($N = 383$) and 0.58‰ ($N = 325$), respectively.

1. Introduction

Barite is a sulfate mineral with extremely low solubility ($K_{sp} \approx 10^{-10}$) and remarkable chemical stability.[1,2] It can be found in a wide array of geological environments and reservoirs, including sedimentary, metamorphic, and igneous rocks, covering a substantial span of geological time from the Early Archean (~3.5 Ga) to the present.[2,3] The oxygen isotope compositions of barite are widely utilized in Earth science research. One significant application is to track and understand changes in paleo-oceanic redox conditions.[4–6] Furthermore, when combined with sulfur isotopes, the oxygen isotope compositions of barite aid in examining the genesis of sulfide and layered barite deposits.[7,8] Additionally, they offer valuable insights into reconstructing sulfate reduction rates and concentrations in ancient oceans, shedding light on past environmental dynamics.[9,10]

The oxygen isotope compositions of barite are typically measured using either a conventional temperature conversion elemental analyzer (TCEA) with IRMS or SIMS.[11–13] SIMS is a preferred choice for isotope microanalysis due to its ability to perform *in situ* measurements with high spatial resolution down to micrometer levels. To ensure accurate and precise microanalysis, it is crucial to use a high-quality reference material to correct for instrumental mass fractionation (IMF).[15,16] In early studies, an in-house barite reference material (S0327) was used to correct for IMF during barite oxygen isotope microanalysis.[12–14] However, it is difficult to verify the accuracy of the data due to the lack of more reference materials. Recently, Li *et al.* (2024) attempted to provide three barite reference materials (ROM-14898, ROM-48628, and ROM-16921) for inter-laboratory data comparison.[17] Additionally, several factors can potentially affect SIMS oxygen isotope measurements, such as orientation, topography and X–Y effects.[18–20] Careful sample preparation with limited surface relief can efficiently overcome topography and X–Y effects.[19,20] However, there is currently a lack of rigorous investigations regarding the orientation effect for barite.

In this study, we present two new barite reference materials, NJU-Ba-1 and FJ, for SIMS oxygen isotope analysis. We investigated the crystallographic orientation effect on SIMS barite oxygen isotope analyses and evaluated the topography and X–Y effect based on meticulous sample preparation. Electron probe microanalysis (EPMA) data suggest the chemical homogeneity of the major elements in the two barite references. The $\delta^{18}O_{VSMOW}$ values of NJU-Ba-1 and FJ were determined using GS-

[a]State Key Laboratory for Mineral Deposits Research, School of Earth Sciences and Engineering, Nanjing University, Nanjing 210023, China

[b]International Center for Isotope Effects Research, Nanjing University, Nanjing 210023, China. E-mail: wxl@nju.edu.cn

† Electronic supplementary information (ESI) available. See DOI: https://doi.org/10.1039/d3ja00353a

IRMS. Multiple sessions of SIMS analyses suggest the oxygen isotope homogeneity of NJU-Ba-1 and FJ, confirming their potential as two microanalysis reference materials for barite oxygen isotopes.

2. Sample description and preparation

The materials investigated in this study are two natural barite samples, NJU-Ba-1 and FJ. The former was collected from barite veins in Xiaogang Village, Fengyang County, Anhui Province, China (Fig. 1). The collected NJU-Ba-1 sample consists mostly of barite with some pyrite on the margins and trace carbonate inclusions. Approximately 800 g of the NJU-Ba-1 barite vein was crushed and sieved, after which the barite fragments were handpicked under a binocular microscope. Verified by backscattered electron imaging (BSE; Fig. S1†), the handpicked barite fragments have high purity without any other impurities. The total mass of the handpicked pure barite fragments is approximately 500 g. The other sample FJ is a pure barite mineral from Fujian Province, China. It has been recently characterized as a barite reference material for barium isotope measurements using LA-MC-ICP-MS (for more detailed information, please refer to Zhang *et al.*, 2022).[21]

For this study, approximately 146 NJU-Ba-1 and 120 FJ barite fragments, each with a diameter of 0.05–0.4 mm (BSE; Fig. S1†), were randomly selected and mounted in epoxy resin to form 25.4 mm disks. The fragments were mounted at the center (15 mm in diameter) of the disk. To achieve a smooth surface for SIMS analysis, grains were abraded using silicon carbide abrasive paper with particle sizes of 5 μm, 2.7 μm, and 1.25 μm successively, followed by polishing with a diamond polishing suspension with particle sizes of 3 μm and 1 μm, respectively. Subsequently, a carbon coating (~20 nm thick) for EPMA analysis and a gold coating (~30 nm thick) for SIMS analysis were applied to the mount as a conductive layer.

To evaluate the crystallographic orientation effect of barite during SIMS oxygen isotope analysis, one NJU-Ba-1 barite mount was subjected to electron backscatter diffraction (EBSD) analysis. For EBSD analysis, the surface layer needs to be damage free. To obtain a good-quality surface, the mount was further polished with a diamond polishing suspension with a diameter of 0.5 μm and 0.3 μm successively, followed by chemical polishing using a VibroMet2 vibratory polisher with an alumina polishing suspension with a diameter of 0.05 μm and a 0.02 μm non-crystallizing colloidal silica polishing suspension. Subsequently, a thin carbon coating (~10 nm thick) was applied on the mount.

Some NJU-Ba-1 and FJ barite fragments were ground to a powder (<75 μm) and prepared for bulk analysis. To investigate the impact of trace amounts of carbonate inclusions on the bulk analysis of the barite oxygen isotopes, four parts of the NJU-Ba-1 powders were immersed in 1 mol L^{-1} acetic acid solution (HAc) for 48 hours. Intermittent shaking was carried out during the soaking period. Afterward, the powders were rinsed three times with 18.2 MΩ cm ultra-pure water and subsequently dried. For comparison, another set of barite powders was used without any chemical treatment.

Fig. 1 Photograph of NJU-Ba-1 barite collected from barite veins in Xiaogang Village, Fengyang County, Anhui Province.

3. Analytical techniques

3.1. EPMA

Mineral element analysis was conducted at the State Key Laboratory for Mineral Deposits Research, Nanjing University, China. The qualitative element analyses of NJU-Ba-1 and FJ were performed using a JEOL-JXA-8230 Plus EPMA at a 15 kV accelerating voltage, and 50 nA beam current. The wavelengths were scanned from 70 to 230 mm, with a 50 μm step size and 100 ms dwell time for each point.

The major element composition and elemental mapping analyses of NJU-Ba-1 and FJ were performed using a JEOL-JXA-8530F EPMA. The analytical conditions for major element composition analysis were set at a 15 kV accelerating voltage, a 20 nA beam current and a 5 μm beam size. The peak counting times were set to 10 s for all major elements. The reference materials used for data correction were barite for BaO and SO_3; amphibole for CaO, MgO and FeO; crocoite for PbO; chalcopyrite for CuO; and celestite for SrO. Elemental mapping was performed at a 15 kV accelerating voltage, 50 nA beam current, 0.3 μm step size and 10 ms dwell time for each point.

3.2. EBSD

EBSD was conducted at the School of Earth Sciences and Engineering, Nanjing University, China. EBSD analyses of NJU-Ba-1 barite fragments were performed using a Tescan Mira 3 XMU field emission scanning electron microscope (SEM) equipped with an Oxford Instruments Nordlys EBSD detector at the FiLTER facility. Lattice preferred orientation (LPO) patterns were acquired with a 70° tilted sample geometry, 20 kV accelerating voltage, and 18–22 mm working distance with a step size of 3.5 μm. Diffraction patterns were automatically indexed using Aztec software (Oxford Instruments). The data were processed and plotted with Aztec Crystal software version 3.1 (Oxford Instruments). Crystallographic orientation maps and

pole figure maps of the analyzed barite fragments were generated to illustrate the orientation of the barite fragments with respect to the major poles (100, 010, and 001) of the stereographic triangle.

3.3. GS-IRMS

GS-IRMS was conducted at the International Center for Isotope Effects Research, Nanjing University, China. Approximately 0.2 mg of barite was loaded into a silver capsule. The capsule was dropped through a zero-blank autosampler (Costech) into a graphite oven heated to 1450 °C. Carbon monoxide (CO) and other gases were produced and then carried by helium gas at a flow rate of 85 mL min^{-1}. The samples were subsequently separated by using a gas chromatograph (GC) at 85 °C and the $\delta^{18}O$ values of sulfate were measured against the reference gas through a conflo-III interface on a Delta V Plus. The $\delta^{18}O$ values are calibrated against the laboratory inhouse reference material ICIER-SO-3 (MERYER-$BaSO_4$) with an assigned $\delta^{18}O_{VSMOW}$ value of 11.8‰.

3.4. SIMS

The SIMS oxygen isotope analysis was conducted using a CAMECA IMS 1300-HR^3 instrument at the State Key Laboratory for Mineral Deposits Research, Nanjing University, China. The key analytical parameters are summarized in Table 1. A primary $^{133}Cs^+$ ion beam (20 keV total impact energy) was focused in Gaussian mode. The 10 μm raster mode was used in the analytical process to reduce the ablation depth, and a normal-incidence electron gun was used for charge compensation. NMR field sensors were applied to stabilize the magnetic field. The magnification of the transfer system was configured as ×75 to increase ion transmission. The ^{16}O and ^{18}O signals were collected simultaneously using two Faraday cups at positions L′2 (10^{10} Ω) and H′2 (10^{11} Ω), respectively. The total analytical time was approximately 4 min per pit: 80 s of pre-sputtering (to remove the gold coating), ~60 s of automatic centering of the secondary ions in the field aperture, and a total of 80 s of integration of secondary ions (20 cycles × 4 s). To minimize the effect of FC noise and ensure precise measurements, FC yield and baseline were calibrated weekly throughout the analysis process. The typical count rates were ~3×10^9 cps for $^{16}O^-$ and ~6×10^6 cps for $^{18}O^-$, and the internal precision for one spot analysis of the oxygen isotope ($^{18}O/^{16}O$ ratio) was typically ~0.2‰ (2SE). The uncertainty from the thermal noise of the Faraday cup (~800 cps for ^{18}O and ~11 000 cps for ^{16}O) was ~0.13‰, and the counting noise (Poisson error) of $^{18}O/^{16}O$ calculated from the instrument was ~0.05‰. The total uncertainty from the FC noise and counting noise was ~0.14‰, consistent with the internal precision of the oxygen isotope measurements.

Table 1 Operating conditions for SIMS analysis of $\delta^{18}O$ of barite

Cs probe diameter (μm)	10
Beam current (nA)	0.8–2.0
Electron gun current (μA)	~0.6
Raster size start (μm)	20
Raster size end (μm)	10
Entrance slit (μm)	~120
Contrast apertures (μm)	400
Field apertures (μm)	6000
Max area (μm)	~107
Transfer optics magnification (8000/max area)	×75
Energy slit (eV)	50–60
Exit slit (μm)	500
MRP, $M/\Delta M$ (50% peak width)	~2500
Detectors	L′2 (FC, 10^{10} Ω) H′2 (FC, 10^{11} Ω)
Secondary ions detected and mean count/s	$^{16}O^- = 1.2 \times 10^9$ to 3.2×10^9 $^{18}O^- = 1.2 \times 10^6$ to 6.0×10^6

The measured $^{18}O/^{16}O$ ratios were converted to $\delta^{18}O$ values by normalizing the measured $^{18}O/^{16}O$ ratios to that of the Vienna Standard Mean Ocean Water (0.0020052) as follows:

$$\delta^{18}O_{raw} = \left[\frac{\left(\frac{^{18}O}{^{16}O}\right)_{measured}}{0.0020052} - 1\right] \times 1000 \ (‰) \quad (1)$$

As stated above, robust SIMS analysis requires the correction of IMF. This correction was achieved by analyzing reference materials that matched the matrix of the unknown samples. The IMF factor was quantified through replicate analysis of NJU-Ba-1 barite as follows:

$$IMF = \left(\frac{^{18}O}{^{16}O}\right)_{RM\ measured} \Big/ \left(\frac{^{18}O}{^{16}O}\right)_{RM\ recommended} \quad (2)$$

Once the IMF was obtained, the $\delta^{18}O_{VSMOW}$ values of the samples were calculated using the following equations:

$$\left(\frac{^{18}O}{^{16}O}\right)_{Sample} = \left(\frac{^{18}O}{^{16}O}\right)_{measured} \Big/ IMF \quad (3)$$

$$\delta^{18}O_{VSMOW} = \left[\frac{\left(\frac{^{18}O}{^{16}O}\right)_{Sample}}{0.0020052} - 1\right] \times 1000 \ (‰) \quad (4)$$

There are a total of fifteen sessions for SIMS oxygen isotope analysis of FJ and NJU-Ba-1 barite. Each session includes analyses of 3–41 fragments, and there are 1–16 spot analyses for each fragment. The homogeneity of the oxygen isotope ratios in two barite materials (NJU-Ba-1 and FJ) was examined. The influences of crystallographic orientation, topography, and the *X*–*Y* position on SIMS oxygen isotopes were investigated. Additionally, to evaluate the stability of the instrument in this study, two well characterized zircon reference materials (Penglai and Qinghu) were analyzed intermittently throughout the fifteen sessions.

4. Results and discussion

4.1. Major element compositions of the barite references

The EPMA results suggest that BaO and SO_3 are the main elements of NJU-Ba-1 and FJ (Fig. S2, S3 and Table S2†). NJU-Ba-1 is composed of 34.8 ± 0.2 wt% SO_3, 64.8 ± 0.2 wt% BaO, 0.04 ± 0.02 wt% SrO, 0.01 ± 0.01 wt% CaO, 0.02 ± 0.02 wt% FeO, 0.02 ± 0.03 wt% CuO, and 0.008 ± 0.005 wt% MgO. FJ is composed of 35.2 ± 0.2 wt% SO_3, 64.6 ± 0.1 wt% BaO, 0.02 ± 0.01 wt% CaO, 0.02 ± 0.03 wt% FeO, and 0.05 ± 0.03 wt% CuO, and its MgO and SrO contents are mostly below the detection limits (0.003 wt% for MgO; 0.006 wt% for SrO) (Table 2). The results from different portions of the two barite fragments show spatial consistency in major element mappings without internal zoning (Fig. 2), which suggests that both barites are homogenous at the micrometer scale for major element contents.

Table 2 EPMA measurement results for major elements (wt%) in NJU-Ba-1 and FJ barite

Sample#	SO_3	BaO	SrO	CaO	PbO	MgO	FeO	CuO	Total
NJU-Ba-1	34.8	64.9	0.04	—	—	0.014	—	0.07	99.8
NJU-Ba-1	35.0	65.1	0.03	—	—	—	—	—	100.1
NJU-Ba-1	34.9	64.7	0.08	0.01	—	0.003	0.05	—	99.7
NJU-Ba-1	34.6	64.7	0.04	0.01	—	0.004	—	—	99.4
NJU-Ba-1	34.9	64.5	0.03	0.03	—	0.009	0.03	0.01	99.5
Mean	**34.8**	**64.8**	**0.04**	**0.01**	**—**	**0.008**	**0.04**	**0.04**	**99.7**
1SD	**0.2**	**0.2**	**0.02**	**0.01**	**—**	**0.005**	**0.01**	**0.04**	**0.3**
FJ	35.3	64.4	—	0.02	—	—	0.01	—	99.7
FJ	35.2	64.4	—	0.03	—	—	0.01	—	99.6
FJ	35.3	64.7	—	—	—	—	0.06	0.07	100.1
FJ	34.9	64.5	—	0.01	—	—	0.01	0.06	99.5
FJ	35.1	64.8	0.01	—	—	0.006	—	0.01	99.9
Mean	**35.2**	**64.6**	**0.01**	**0.02**	**—**	**0.006**	**0.02**	**0.05**	**99.8**
1SD	**0.2**	**0.2**	**—**	**0.01**	**—**	**—**	**0.03**	**0.03**	**0.3**

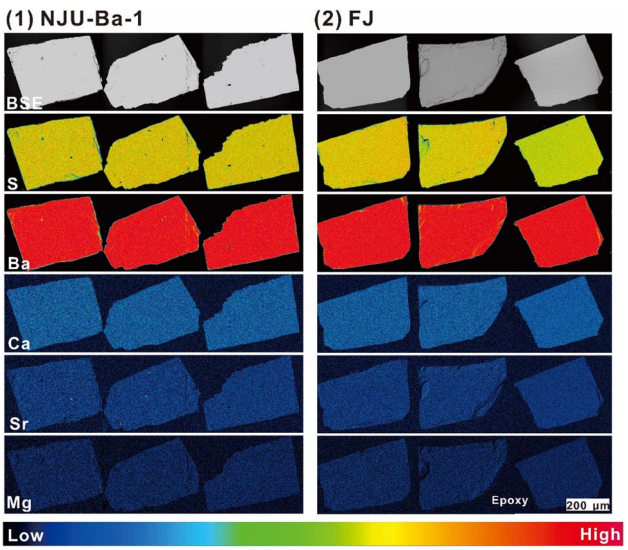

Fig. 2 BSE imaging and major elemental mapping of NJU-Ba-1 and FJ barite. Data are available in Table 2.

4.2. GS-IRMS $\delta^{18}O$ values of NJU-Ba-1 and FJ

The detailed results of the bulk oxygen isotope compositions of NJU-Ba-1 and FJ barite powders are given in Table 3 and Fig. 3. This high-temperature conversion plus elemental analyzer approach achieved a precision of ± 0.3‰ (2SD, $N = 13$) for the $\delta^{18}O$ value of replicate analyses of ICIER-SO-3 (Table 3). The analysis was repeated eleven times for NJU-Ba-1 and eight times for FJ, with average $\delta^{18}O_{VSMOW}$ values of 7.94 ± 0.30‰ (2SD, $N = 11$) and 7.52 ± 0.34‰ (2SD, $N = 8$), respectively.

To investigate the influence of tiny carbonate inclusions on the bulk analyses, two sets of experiments were conducted in

Table 3 Summary of GS-IRMS results for the oxygen isotope values of NJU-Ba-1 and FJ barites

Sample #	$\delta^{18}O$ (‰, VSMOW)
NJU-Ba-1	7.88
NJU-Ba-1	8.16
NJU-Ba-1	7.86
NJU-Ba-1	7.90
NJU-Ba-1	8.15
NJU-Ba-1	8.04
NJU-Ba-1	7.94
Mean	**7.99 ± 0.25 (2SD, $N = 7$)**
NJU-Ba-1[a]	7.69
NJU-Ba-1[a]	8.09
NJU-Ba-1[a]	7.81
NJU-Ba-1[a]	7.83
Mean[a]	**7.85 ± 0.34 (2SD, $N = 4$)**
Mean (all NJU-Ba-1)	**7.94 ± 0.30 (2SD, $N = 11$)**
FJ	7.70
FJ	7.39
FJ	7.66
FJ	7.65
FJ	7.41
FJ	7.69
FJ	7.25
FJ	7.41
Mean	**7.52 ± 0.34 (2SD, $N = 8$)**
Reference material (ICIER-SO-3)	**11.81 ± 0.30 (2SD, $N = 13$)**

[a] Barite powder is treated with HAC.

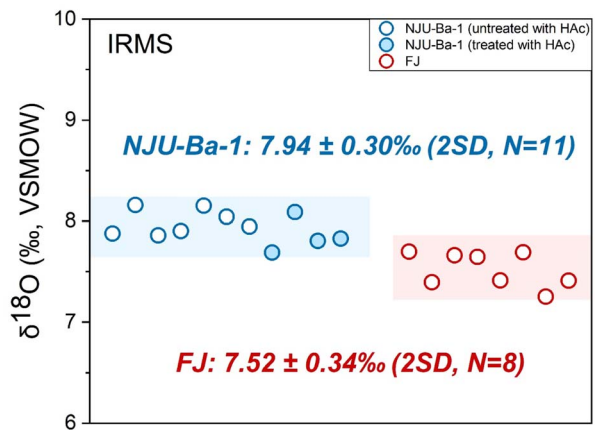

Fig. 3 Isotope ratio mass spectrometry $\delta^{18}O_{VSMOW}$ results of NJU-Ba-1 and FJ barites. Data are available in Table 3.

this study (Fig. 3 and Table 3). One group of NJU-Ba-1 barite powders was treated with 1 mol L^{-1} HAc to dissolve carbonates before bulk analysis. For comparison, another group of NJU-Ba-1 barite powders were directly analyzed by GS-IRMS without HAc treatment. The mean $\delta^{18}O_{VSMOW}$ values obtained from the two groups were 7.85 ± 0.34‰ (2SD, $N = 4$) and 7.99 ± 0.25‰ (2SD, $N = 7$). Statistical analysis using Student's *t*-test revealed that there is no significant difference between the two groups, with a *p*-value of 0.164 (>0.05). This indicates a high level of confidence in the consistency of the mean values obtained with and without HAc treatment. This consistency suggests that the presence of tiny carbonate inclusions has a negligible influence on the bulk oxygen isotope analysis of the barite sample. Hence, the mean $\delta^{18}O_{VSMOW}$ value of the two groups, 7.94 ± 0.30‰ (2SD, $N = 11$), was utilized to correct the IMF during the SIMS analysis.

4.3. SIMS

All the SIMS analyses are listed in Tables S2 and S3.† To achieve accurate and precise SIMS analysis of barite oxygen isotopes, the following four aspects need to be carefully examined: (1) accuracy and precision of the analytical process, (2) orientation effect, (3) *X*–*Y* position effect, and (4) homogeneity of reference materials.

4.3.1 Accuracy and precision. Instrumental stability is crucial to obtain highly accurate and precise $\delta^{18}O$ values. In this study, oxygen isotopes of Penglai and Qinghu zircon reference materials were analyzed intermittently to assess the instrumental stability during the barite $\delta^{18}O$ measurements. The data are shown in Table S1† and Fig. 4. Penglai zircon was used as the bracketing standard to correct for IMF during zircon analysis, which produced a two standard deviation value of 0.23‰ ($N = 66$; Fig. 4). The corrected mean $\delta^{18}O_{VSMOW}$ value for Qinghu zircon was 5.53 ± 0.27‰ (2SD, $N = 35$), which is consistent with its reference value (5.39 ± 0.22‰, 2SD).[22] These

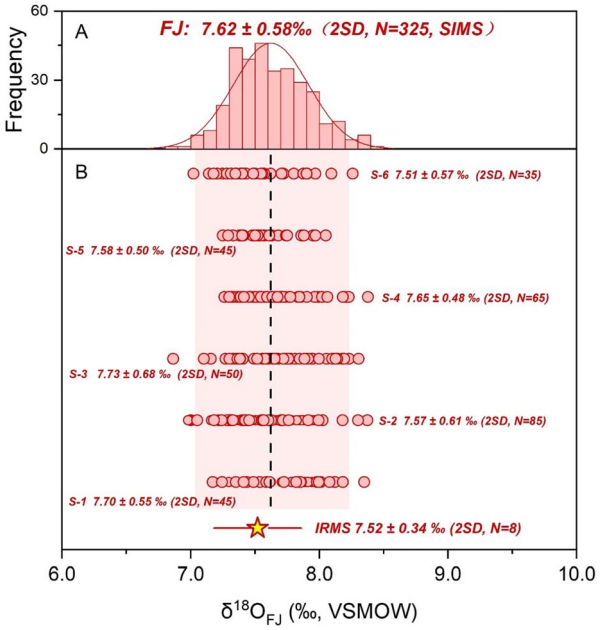

Fig. 5 Distribution pattern (A) and corrected $\delta^{18}O_{VSMOW}$ values (B) of FJ barite. NJU-Ba-1 barite was used as a bracketing standard to correct for IMF and the $\delta^{18}O_{VSMOW}$ value of NJU-Ba-1 measured by GS-IRMS is 7.94 ± 0.30‰ (2SD, $N = 11$, Table 3). Data are available in Table S2.†

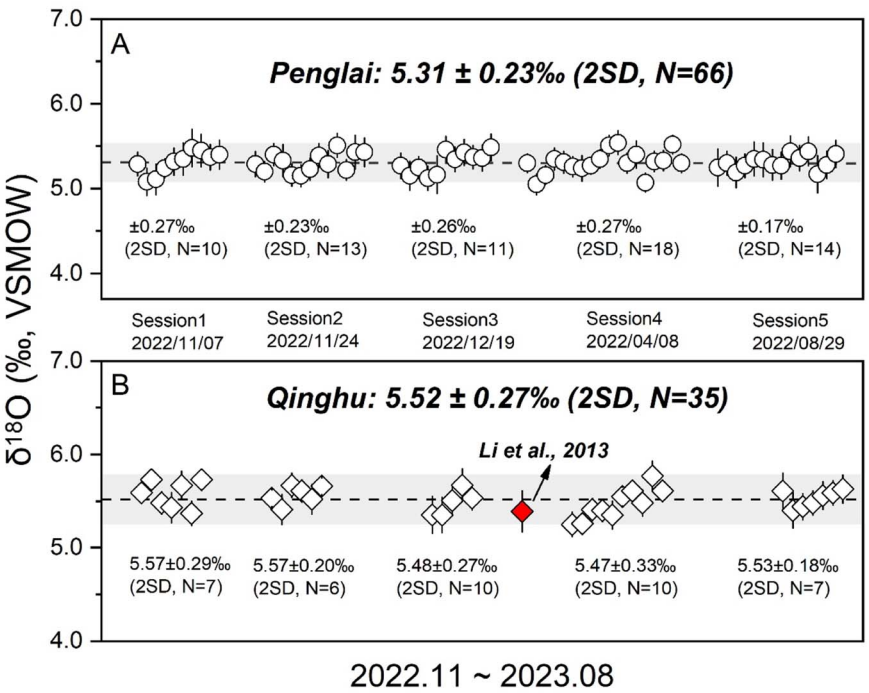

Fig. 4 Corrected oxygen isotope results for Penglai zircon (A) and Qinghu zircon (A) reference materials. Data are available in Table S1.†

results demonstrate the good stability of the instrument during the measurement processes.

The accuracy of the barite SIMS oxygen isotope analysis was verified by comparing the SIMS data with the values measured by GS-IRMS. NJU-Ba-1 barite was used as a bracketing standard to correct for IMF and to further monitor the stability of the instrument during SIMS analysis. For each session, NJU-Ba-1 was analyzed once for every five measurements of FJ. The $\delta^{18}O_{VSMOW}$ value of the NJU-Ba-1 barite used for IMF correction was 7.94 ± 0.30‰. The corrected $\delta^{18}O_{VSMOW}$ value of FJ barite was 7.62 ± 0.58‰ (2SD, $N = 325$; Table S2† and Fig. 5), which is consistent with the values measured by GS-IRMS (7.52 ± 0.34‰, 2SD, $N = 8$). Furthermore, the $\delta^{18}O$ variation in NJU-Ba-1 in each session measured by SIMS was <0.3‰ (2SD, Table S2†), further indicating the high stability of the instrument. In conclusion, our SIMS method can accurately and precisely analyze the barite oxygen isotope compositions.

4.3.2 Lack of orientation effect for barite SIMS oxygen isotope analysis. The orientation effect can present significant challenges for achieving accurate and precise SIMS oxygen isotope analysis. For instance, orientation effects in SIMS magnetite $\delta^{18}O$ analysis can result in a variation of up to 2.9‰.[18] This deviation is large enough to affect analysis since the typical precision of routine SIMS $\delta^{18}O$ analysis is better than 0.3‰.[23,24] Consequently, it is imperative to investigate and minimize orientation effects to ensure reliable and precise measurement results.

In this study, NJU-Ba-1 and FJ barite fragments were randomly mounted in epoxy resin for SIMS analysis to obtain a random crystallographic orientation. However, it is important to note that barite has a perfect cleavage along the (001) plane, which means that fragments tend to lie on these cleavage faces. Consequently, during the mounting process, there is a greater likelihood of a preferential orientation along the long axis

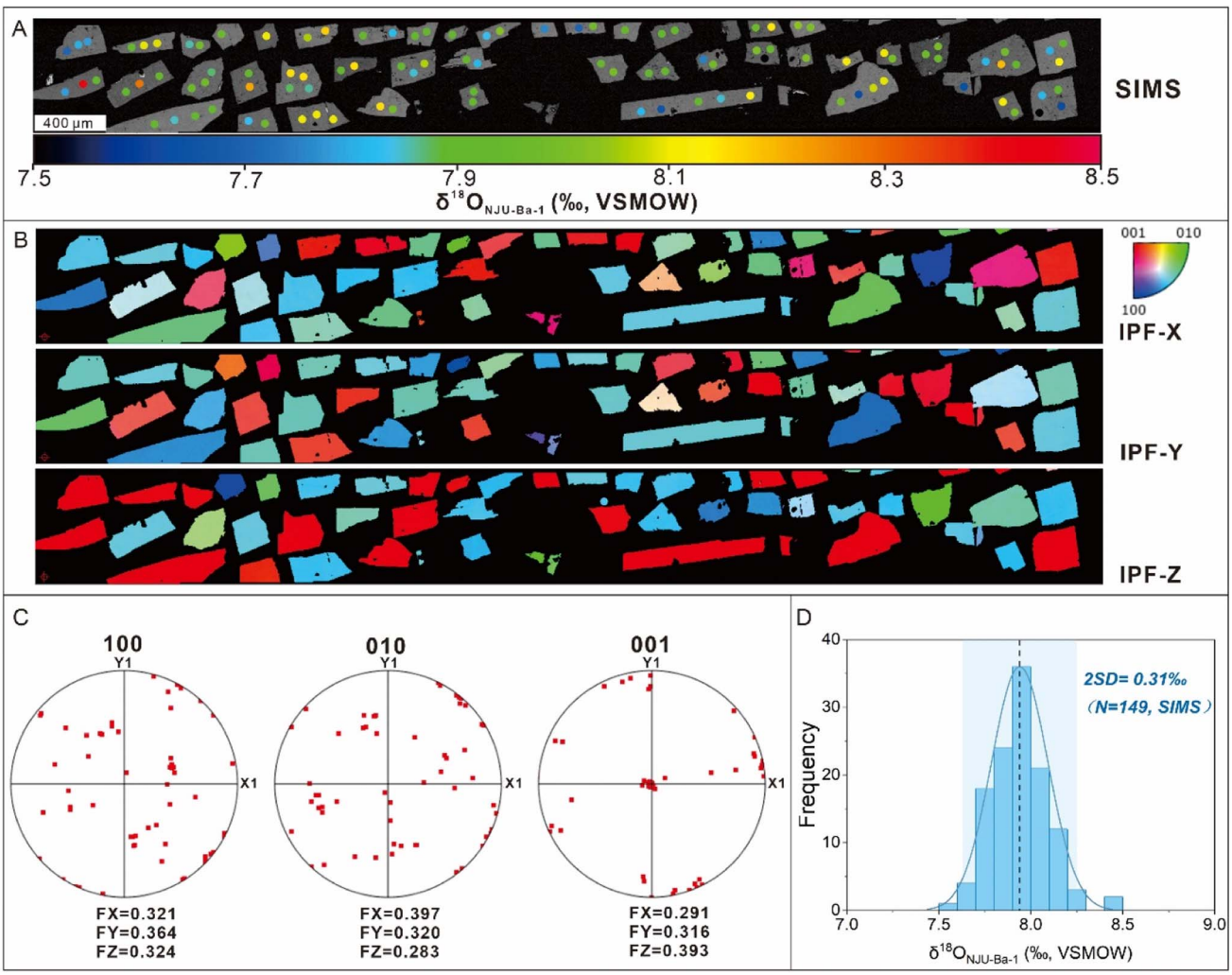

Fig. 6 Evaluating orientation effects of SIMS barite oxygen isotope analysis. (A) SIMS $\delta^{18}O$ values of NJU-Ba-1 barite (sessions 9–11); a color scheme is used to correlate $\delta^{18}O$ values with their analytical positions; (B) crystallographic orientation maps for the studied NJU-Ba-1 barite fragments; (C) pole figure maps of NJU-Ba-1barite fragments; (D) SIMS $\delta^{18}O$ values of NJU-Ba-1 barite displayed as a histogram. No correlation between measured $\delta^{18}O$ values and their crystallographic orientations indicates a lack of orientation effect for SIMS barite oxygen isotope analysis.

parallel to the mount surface. To avoid such defects inherited from sample preparation when evaluating the crystallographic orientation effect, we used EBSD to analyze the crystallographic orientation of 57 NJU-Ba-1 barite fragments. The crystallographic orientation maps and pole figure maps of 57 barite fragments demonstrated a wide range of crystal orientations (Fig. 6B and C). Furthermore, the two standard deviations of 149 spots of 57 NJU-Ba-1 fragments in $\delta^{18}O_{VSMOW}$ were 0.31‰ (N = 149, sessions 6–8, Fig. 6A and D). These findings suggest that there are no significant orientation-related biases in the SIMS barite oxygen isotope analysis under current analytical precision, which is consistent with the results reported by Magnall *et al.* (2016) and Li *et al.* (2024).[12,17]

4.3.3 No significant topography and *X*–*Y* effect in barite SIMS oxygen isotope analysis. The surface topography of the mounts and the location of the primary beam impact within the sample holder window (*X*–*Y* effects) can introduce significant instrumental artifacts during analysis.[19,20,25–27] Both topography and *X*–*Y* effects are probably due to a deformation of the electrostatic field (−10 kV) that could displace the secondary beam trajectory and overall result in bias in the oxygen isotope ratio.[19] For CAMECA IMS-1300 HR^3 SIMS, beam centering parameters DTFA-*X*, DTFA-*Y*, DTCA-*X*, and DTCA-*Y* form double deflection transfer centering on the trajectory of secondary ions in the field aperture (FA) and contrast aperture (CA).[20] DTCA often reflects the surface relief effect and DTFA often reflects the mount surface height change.[15,20] Therefore, instrumental tuning parameters DTCA and DTFA have been utilized to identify potential causes of instrumental bias, such as surface topography, tilting or stray magnetic fields.[28]

For topography related artifacts, careful sample preparation with a limited polishing relief of less than a few micrometers can efficiently overcome these effects.[19,20] Through meticulous sample preparation in this study, surface relief was quantified to be less than 3 μm using contact stylus profilometry (Fig. S4 and S5†). The observed data did not show significant correlation between DTCA *XY* and $\delta^{18}O$. These results suggest that there is no significant influence of topography on our analytical results.

X–*Y* effects are analytical artifacts resulting from the sample topography and location on the sample stage.[19] Large geometric artifacts on SIMS oxygen isotope analysis have been reported from various laboratories.[19,20,25–27] To obtain high quality data, there are several recommendations from previous studies, *e.g.* obtaining a flat mount surface, confining sample grains within the center of the mount, using a large front surface sample holder, and ensuring proper placement of calibration standards.[19,20,25–27] This study followed the above principles, and the results revealed no significant changes in oxygen isotope ratios in the *X* or *Y* directions (Tables S2 and S3†).

4.3.4 Homogenous oxygen isotope compositions of NJU-Ba-1 and FJ barite. It is critical to develop homogenous reference materials for *in situ* analysis. In this study, a comprehensive investigation was conducted to assess the oxygen isotope homogeneity of both NJU-Ba-1 and FJ barite materials over ten months. The SIMS results for 146 NJU-Ba-1 barite fragments from nine sessions are presented in Fig. 7 and Table S3.† All the

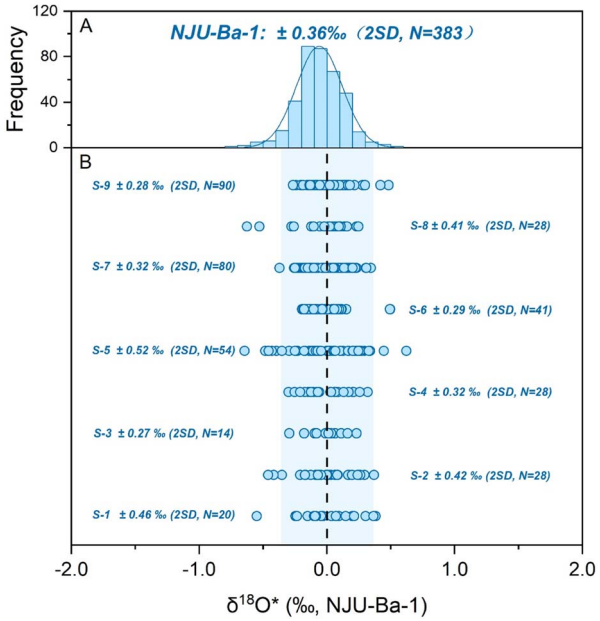

Fig. 7 Distribution pattern (A) and two standard deviations (B) of NJU-Ba-1 barite. $\delta^{18}O^*$ represents $^{18}O/^{16}O_{NJU\text{-}Ba\text{-}1}$ normalized to average $^{18}O/^{16}O_{NJU\text{-}Ba\text{-}1}$ in each session. Data are available in Table S3.†

individual analysis results of NJU-Ba-1 are consistent and yield a Gaussian distribution with two standard deviations of 0.36‰ (N = 383, Fig. 7A). The results demonstrate a high level of long-term reproducibility. According to ISO Guide 35-2017, the $\delta^{18}O$ variation in NJU-Ba-1 barite between different fragments (inter-unit variation) and within a single fragment (intra-unit variation) was examined.[29] In total, 86 spots were analyzed from 21 random NJU-Ba-1 fragments (Table S4†). The results reveal that the inter-unit variance of NJU-Ba-1 was ± 0.19‰ (2SD; Table S6†), and the intra-unit variance of NJU-Ba was ±0.33‰ (2SD; Table S6†). Such small variations indicate that the oxygen isotopes of NJU-Ba-1 display a homogeneous distribution and it has potential to be a reference material.

The SIMS results for 120 FJ barite fragments from all six sessions are presented in Fig. 5 and Table S2.† In these sessions, bracketing standard NJU-Ba-1 barite was analyzed once for every five FJ analyses. All the individual analysis results of FJ also yield a Gaussian distribution with two standard deviations of 0.58‰ (N = 325; Fig. 5). Similarly, FJ barite was examined for variation between different fragments and within a single fragment.[29] In total, 16 FJ fragments were randomly selected, and 110 spots were examined (Table S5†). The results show that the inter-unit variance of FJ was ±0.29‰ (2SD; Table S6†), and the intra-unit variance of FJ was ±0.40‰ (2SD; Table S6†). These results also exhibit good homogeneity, although the variation is slightly greater than the current measurement precision. Therefore, FJ can be used as an accessory reference material.

5. Conclusions

This study introduces two chemically homogeneous barite reference materials, NJU-Ba-1 and FJ, which are recommended

for precise SIMS oxygen isotope measurements. The $\delta^{18}O_{VSMOW}$ values determined by GS-IRMS are 7.94 ± 0.30‰ (2SD, $N = 11$) for NJU-Ba-1 and 7.52 ± 0.34‰ (2SD, $N = 8$) for FJ. We conducted a systematic investigation into the potential causes of bias in $\delta^{18}O$ values by IMF. The results revealed that there is no significant crystallographic orientation effect at the current analytical precision level (~0.3‰). We performed meticulous sample preparation to ensure that the surface relief is <3 μm. Under these conditions, no significant topography or *X*–*Y* effects were observed. After considering these factors, the SIMS $\delta^{18}O$ value analyses of NJU-Ba-1 and FJ indicated uncertainties of 0.36‰ (2SD, $N = 383$) and 0.58‰ (2SD, $N = 325$), respectively. Furthermore, a sufficient quantity (~500 g) of NJU-Ba-1 barite fragments is available for distribution.

Author contributions

Lan–Lan Tian: conceptualization, methodology, investigation, writing – original draft, writing – review and editing. Yue Guan: investigation. Wen-Li Xie: investigation. Kexin Xu: investigation. Feng-Tai Tong: investigation. Tao Yang: resources and supervision. Yong-Bo Peng: resources and supervision. Xiao-Lei Wang: resources, supervision, funding acquisition, review and editing.

Conflicts of interest

There are no conflicts of interest to declare.

Acknowledgements

This work was supported by the State Key Laboratory for Mineral Deposits Research and the "GeoX" Interdisciplinary Research Funds for the Frontiers Science Center for Critical Earth Material Cycling, Nanjing University (2023300291)". The manuscript benefits from the constructive and helpful comments from two anonymous reviewers. We appreciate Zhaochu Hu for providing the FJ barites, Erkang Qiu and Li Zhang for helping with the EBSD analysis, and Zhen Zeng for constructive discussion.

References

1 A. I. Rushdi, J. McManus and R. W. Collier, Marine barite and celestite saturation in seawater, *Mar. Chem.*, 2000, **69**(1–2), 19–31.
2 J. S. Hanor, *Rev. Mineral. Geochem.*, 2000, **40**(1), 193–275.
3 G. Y. Wei, H. F. Ling, G. A. Shields, S. V. Hohl, T. Yang, Y. B. Lin and F. Zhang, *Geology*, 2021, **49**(9), 1059–1063.
4 W. Yao, A. Paytan and U. G. Wortmann, *Geochim. Cosmochim. Acta*, 2020, **269**, 257–269.
5 S. Markovic, A. Paytan, H. Li and U. G. Wortmann, *Geochim. Cosmochim. Acta*, 2016, **175**, 239–251.
6 A. V. Turchyn and D. P. Schrag, *Earth Planet. Sci. Lett.*, 2006, **241**(3–4), 763–779.
7 S. Sharifiyan, M. R. Hosseinzadeh, S. Maghfouri and M. Moayyed, *Ore Geol. Rev.*, 2021, **139**, 104549.
8 H. K. Hormozi, F. Ehya, G. R. Paydar and S. M. Kheymehsari, *Geochemistry*, 2023, 126024.
9 G. Antler, A. V. Turchyn, S. Ono, O. Sivan and T. Bosak, *Geochim. Cosmochim. Acta*, 2017, **203**, 364–380.
10 S. Gong, D. Feng, Y. Peng, J. Peckmann, X. Wang, Y. Hu, Q. Liang, J. Feng and D. Chen, *Chem. Geol.*, 2021, **581**, 12039.
11 H. Bao, D. Rumble III and D. R. Lowe, *Geochim. Cosmochim. Acta*, 2007, **71**(20), 4868–4879.
12 J. M. Magnall, S. A. Gleeson, R. A. Stern, R. J. Newton, S. W. Poulton and S. Paradis, *Geochim. Cosmochim. Acta*, 2016, **180**, 146–163.
13 H. M. Grema, J. M. Magnall, M. J. Whitehouse, S. A. Gleeson and H. M. Schulz, *Front. Earth Sci.*, 2022, **9**, 784824.
14 R. Weibel, M. J. Whitehouse, M. Olivarius, F. C. Jakobsen, A. Mathiesen, H. H. Midtgaard and M. Larsen, *Sediment. Geol.*, 2022, **428**, 106063.
15 C. Fàbrega, D. Parcerisa, J. M. Rossell, A. Gurenko and C. Franke, *J. Anal. At. Spectrom.*, 2017, **32**(4), 731–748.
16 J. M. Eiler, C. Graham and J. W. Valley, *Chem. Geol.*, 1997, **138**(3–4), 221–244.
17 B. Li, M. Wiedenbeck, F. Couffignal, A. M. Álvarez-Valero, H. M. Bao, C. F. Fan, J. Han, G. S. Jin, Y. B. Peng, M. D. Syczewski, K. T. Tait, F. D. H. Wilke and U. G. Wortmann, *Geostand. Geoanal. Res.*, 2024, **48**(1), 197–205.
18 J. M. Huberty, N. T. Kita, R. Kozdon, P. R. Heck, J. H. Fournelle, M. J. Spicuzza, H. Xu and J. W. Valley, *Chem. Geol.*, 2010, **276**(3–4), 269–283.
19 N. T. Kita, T. Ushikubo, B. Fu and J. W. Valley, *Chem. Geol.*, 2009, **264**(1–4), 43–57.
20 G. Q. Tang, X. H. Li, Q. L. Li, Y. Liu, X. X. Ling and Q. Z. Yin, *J. Anal. At. Spectrom.*, 2015, **30**(4), 950–956.
21 S. Zhang, W. Zhang, H. Yu, F. Huang, C. Wang, T. Luo, Y. Liu and Z. Hu, *J. Anal. At. Spectrom.*, 2022, **37**(12), 2637–2646.
22 X. Li, G. Tang, B. Gong, Y. Yang, K. Hou, Z. Hu, Q. Li, Y. Liu and W. Li, *Chin. Sci. Bull.*, 2013, **58**, 4647–4654.
23 R. B. Ickert and R. A. Stern, *Geostand. Geoanal. Res.*, 2013, **37**(4), 429–448.
24 N. T. Kita, J. M. Huberty, R. Kozdon, B. L. Beard and J. W. Valley, *Surf. Interface Anal.*, 2011, **43**(1-2), 427–431.
25 P. Peres, N. T. Kita, J. W. Valley, F. Fernandes and M. Schuhmacher, *Surf. Interface Anal.*, 2013, **45**(1), 553–556.
26 P. C. Treble, A. K. Schmitt, R. L. Edwards, K. D. McKeegan, T. M. Harrison, M. Grove, H. Cheng and Y. J. Wang, *Chem. Geol.*, 2007, **238**(3–4), 197–212.
27 M. J. Whitehouse and A. A. Nemchin, *Chem. Geol.*, 2009, **261**(1–2), 32–42.
28 M. Schuhmacher, F. Fernandes and E. de Chambost, *Appl. Surf. Sci.*, 2004, **231–232**, 878–882.
29 International Organization of Standardization, *ISO Guide 35*, International Organization of Standardization, Geneva, Switzerland, 2017.

